

# **A NEW WAVE EQUATION FORMULATION WITH A FOCUS ON DEVIATED WELL APPLICATIONS DERIVED FROM DOWNHOLE DYNAMOMETER MEASURED DATA**

Peter Westerkamp and Tom Mills

Lufkin Industries

## **BACKGROUND**

The original algorithm used in automation systems was designed for vertical wells, where subsurface conditions are relatively uniform. However, today's deviated and horizontal wells introduce entirely different angled trajectories which create unique challenges such as gravitational forces and bending forces.

Conventional vertical sucker rod models do not account for Coulomb friction, which arises from mechanical interaction between rods and tubing, guides and tubing, or both.

This paper provides a brief history and overview of the downhole dynamometer project, its initial findings and the resulting initial improved mathematical model and its benefits.

## **PROJECT OBJECTIVES**

The project's objective was to design, build and run downhole dynamometer tools, strategically located in the rod string, to collect and analyze data to better understand the impact of wellbore tortuosity on rod string stresses and side loads, and the impact on the downhole pump card, which is used to control the well. This, to deliver improved design and diagnostic tools to improve rod lift control in deviated wells to lower production costs, extend run life in between failures and improve the efficacy of work overs.

## **PROJECT HISTORY**

The original project began around 2013, GE's acquisition of Lufkin Industries created an opportunity for Lufkin to collaborate with GE's research and development facility in Niskayuna, NY, and later with the GE facility in Oklahoma City, OK. In 2016, the first-generation tools were deployed in New Mexico, albeit with limited success. The tool's 1.89" outer diameter, combined with 2-3/8" tubing, necessitated a complex downhole completion. The pump and downhole dynamometer tool were run into the well with the tubing string, the connection with the rod string was established after several attempts using an on-off tool. Additionally, a third-party downhole dynamometer tool positioned higher in the rod string parted, adding further complications to the first tool run.

The lessons learned from this initial attempt led to significant improvements in both the tool and software design. Tool firmware was enhanced to support a flexible, programmable logging schedule, optimizing the use of available onboard memory. The tool's diameter was reduced from 1.89" to 1.625" to fit 2-3/8" tubing completions, while changes in the tool body metallurgy helped lower manufacturing costs. One tool was subjected to load testing to destruction to demonstrate its load limits for customers.

By 2021, the current generation of the tool design was completed, and since then, 9 more successful tool runs have been completed. For each well, multiple tool runs were performed, with variations in rod string or pump design for each test. Up to 64 ten-minute samples were collected per tool run, with each sample

period pre-programmed to accommodate speed changes between samples. The data collected downhole was synchronized in real-time with surface-collected data. The battery life lasts for approximately three weeks. Once the battery is depleted, the data is preserved in non-volatile memory.

Current tool specifications:

Weight:	27 Lbs
Diameter / Length:	1.625" / 69"
Pressure Range:	0 – 10,000 PSI
Load operation range:	-9,000 to 30,000Lbs
Acceleration range:	+/- 5G, 3 axis
Power Source:	Custom battery
Sampling rates:	Selectable: 10Hz, 50Hz, 100Hz, 150Hz, 200Hz
Typical log schedule:	64 samples of 10 minutes each (Limited by sampling rate and memory).

## PROJECT CHALLENGES

In addition to the usual hardware and software design challenges, operational issues significantly delayed data collection. While well selection was crucial, it was also limited by availability. In collaboration with the operator, criteria such as location, deviation survey, and downhole completion were established to guide the well selection process. Each well scheduled for intervention was then reviewed to identify a suitable match. After the tools were installed, they were programmed to begin data collection several days later, after entering "sleep mode" to ensure the well was pumped off. Once all logs were collected, the tools were retrieved for data download and refurbishment. A second set of tools was then deployed to collect additional data, either with a different rod string or pump design.

In some instances, finding a suitable well took considerable time. Once the tools were installed and the rig moved on to its next scheduled well, factors such as weather or higher-priority well interventions often delayed the opportunity to retrieve the tools in a timely manner. This led to longer-than-planned run times and unanticipated tool wear. However, it is acknowledged that these delays are a natural part of the project and can only be minimized by providing external funding to compensate operators for workover costs and deferred production. Lufkin is deeply grateful for the operators' collaboration in making wells and workover operations available at no cost.

## INITIAL FINDINGS

### Poor Match Between Measured and Modeled Pump Cards

The current standard for commercial rod pump controllers is to use Gibbs'<sup>1</sup> original 1-dimensional damped wave equation (1DDWE) to model pump cards from surface cards. This approach assumes that the well is vertical and that there is no contact between rods and tubing – thus, no Coulomb friction.

Figure 1 depicts the deviation survey for test well B. This well is nearly vertical. The downhole location is within 65 feet of the surface location.

Figure 2 depicts a pump card measured by downhole instruments compared to the 1DDWE analysis of the associated surface card from Well B. The "fat nose" on the 1DDWE card indicates that there is some source of friction in this well which is not being modeled by the 1DDWE. That source is Coulomb friction.

This is an example of how even a slight deviation from vertical can prevent the 1DDWE from accurately modeling the rod dynamics. Although the differences in this example are subtle and do not materially impact quantitative results or control decisions, this example illustrates the impact of Coulomb friction when the well trajectory even slightly non-vertical.

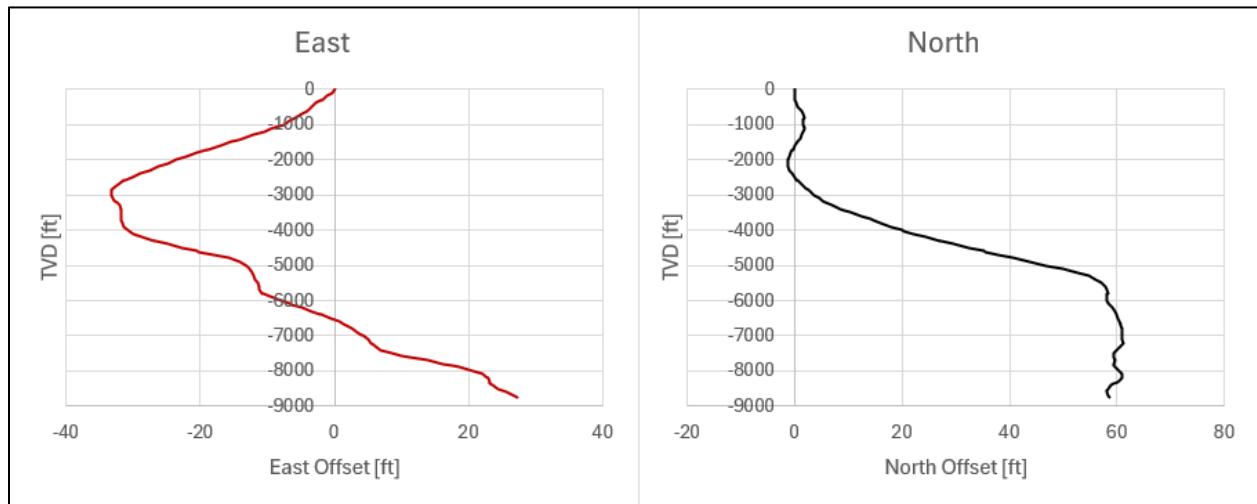


Figure 1: Deviation survey for subject well B

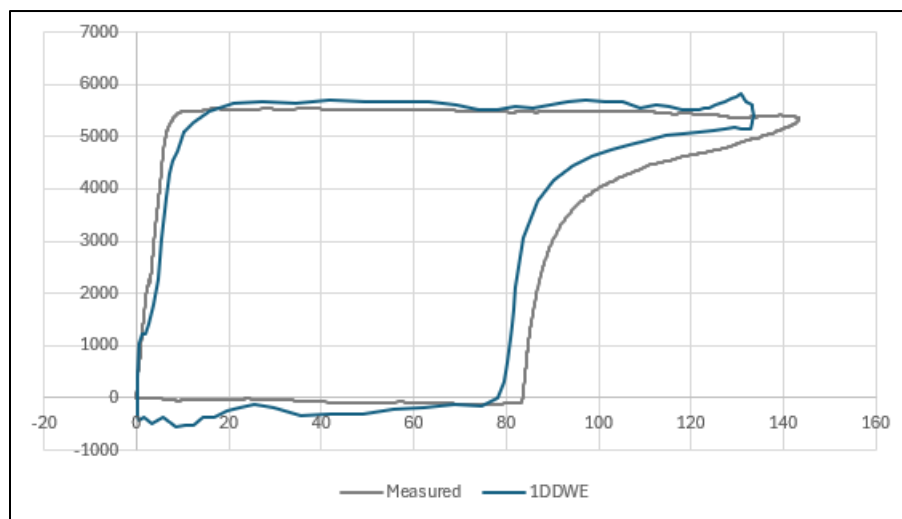


Figure 2: measured and 1DDWE pump cards for test Well B

### Plunger velocity, pump leakage, valve action

The pump cards collected by the downhole instruments revealed some remarkable interactions involving plunger velocity and pump leakage. Although these interactions have been intuitively anticipated and discussed in the literature<sup>2,3</sup>, data were not previously available to quantify them in an operating well.

Figure 3 is typical of the pump cards collected by the downhole instruments. The upstroke of this card has a slight “slant” or “lean to the right” – which might mistakenly be attributed to tubing movement. The middle of the upstroke demonstrates some “humping”/“convexity” – which might incorrectly be attributed to insufficient viscous damping (if the card had been generated by a model). The upper 70% of the upstroke shows a steady decline in fluid load and the final 5% of the upstroke reflects some erratic behavior.

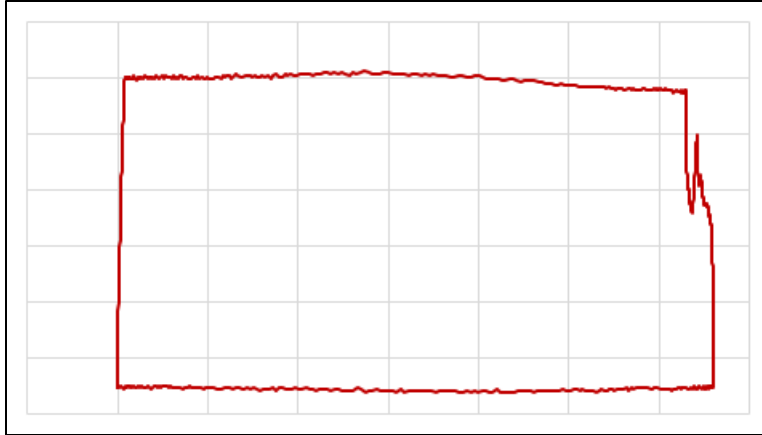


Figure 3: Typical measured pump card

Figure 4 is the (measured) plunger velocity plot for the card in Figure 3. Note that a critical plunger velocity threshold is revealed at the beginning and ending of the upstroke. Until this velocity is reached at the beginning of the upstroke, the traveling valve cannot fully pick up the fluid load. At the top of stroke, as the plunger velocity declines, the traveling valve is having difficulty retaining the fluid load. This explains the anomalous behavior seen in the pump card during the last 5% of the upstroke.

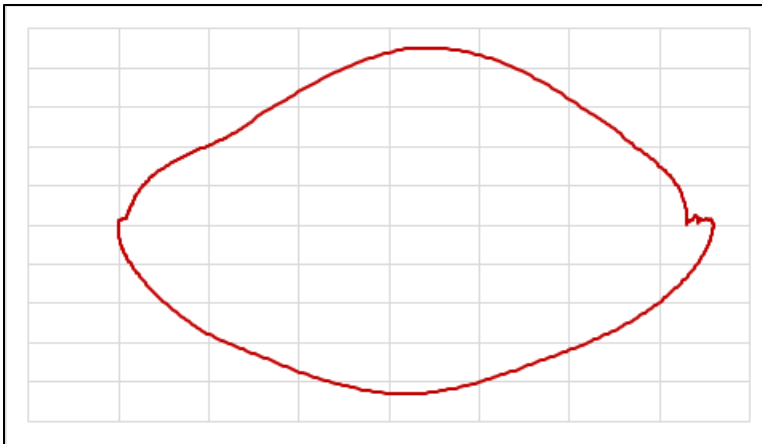


Figure 4: Plunger velocity vs plunger position for card in Figure 2

The humping (convexity) – in the upstroke – is explained by other data collected using the downhole instruments. In addition to recording force and acceleration, the downhole instruments collected pressure (of the surrounding fluid in the tubing). For the downhole instrument located at the pump, the tool is measuring pump discharge pressure. Using the pump discharge pressure and the pump force from the downhole instruments – along with the pump area – pump barrel pressure can be calculated.

Figure 5 is a presentation of calculated pump barrel pressure vs plunger position for the stroke in Figure 3. Note that stroke progression in this plot is “counterclockwise” – starting at the upper-left corner. During the upstroke, the pump barrel pressure collapses from approximately 4500 psia to about 1300 psia as the traveling valve gains the fluid load. From this plot, it appears that pump intake pressure is near 1300 psi.

Figure 6 represents the central portion of the upstroke in Figure 5. The vertical scale is expanded to reveal that during the middle of the stroke – where plunger velocity is highest – the pump barrel pressure drops by approximately 75 psi. This phenomenon is remarkable because it appears that the plunger is vacating the barrel faster than fluid can pass through the standing valve to fill the space. It is even more remarkable given that the pump intake pressure is around 1300 psi. Such behavior may inform pump

component selection. Furthermore, this loss of pressure may raise concerns about gas break-out within the pump during the upstroke.

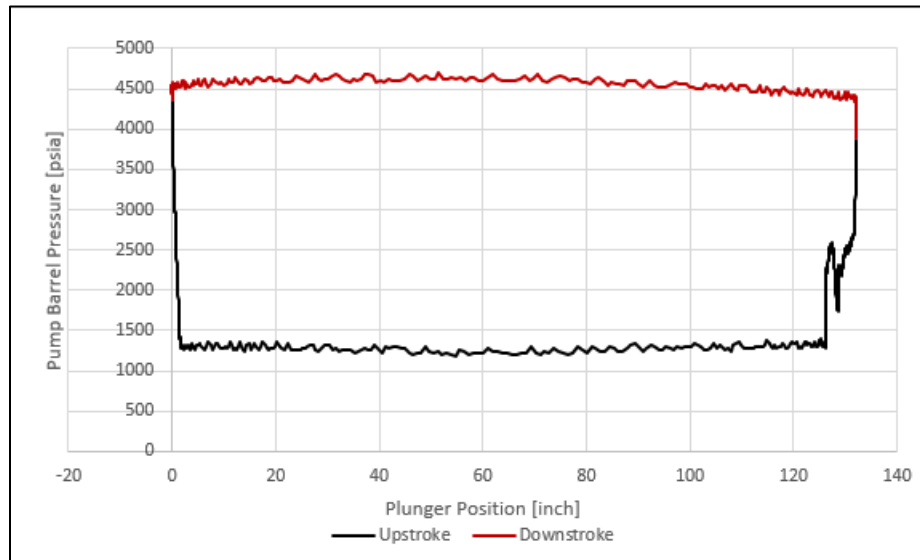


Figure 5: Pump barrel pressure vs plunger position for card in Figure 2

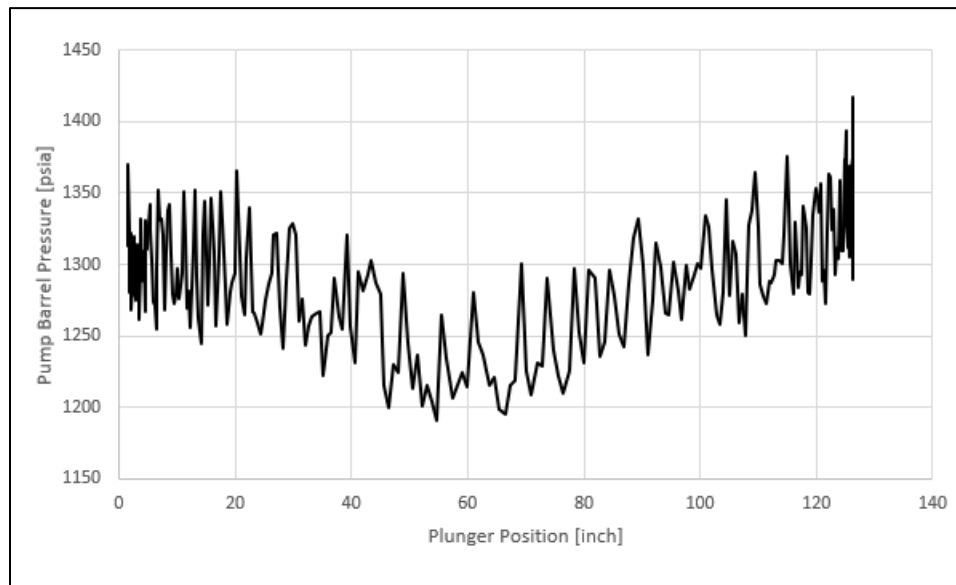


Figure 6: Subsection of Figure 5

Other interesting phenomena were captured by the downhole tools. Figure 7 shows the measured data from the top of stroke from a pump card like the one shown in Figure 3. This enhanced view shows how the load transfer at the top of stroke includes multiple cycles involving complex interaction between rod strain, pump displacement due to surface motion, fluid leakage around the plunger, and fluid inflow through the standing valve. At times, the pump is moving downward (during what would generally be considered upstroke).

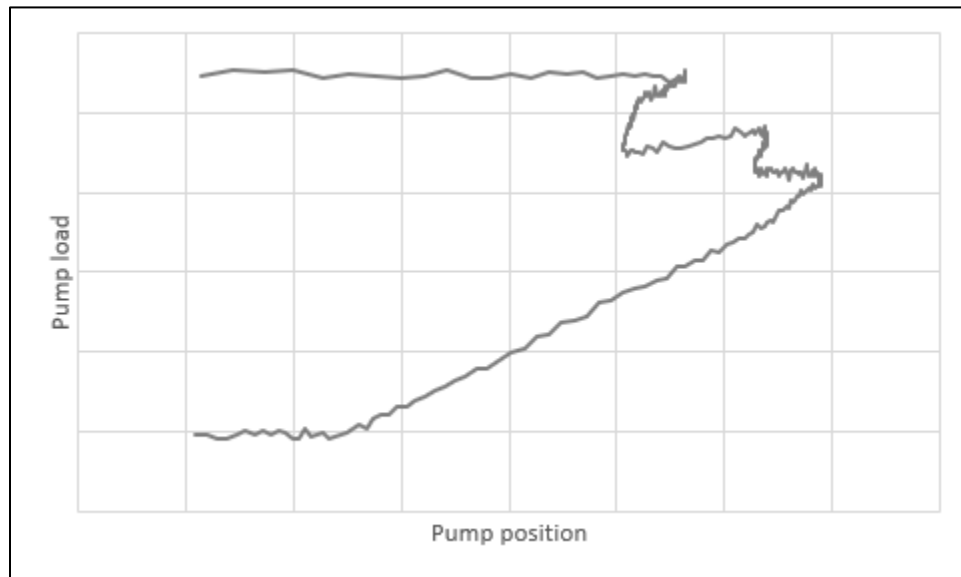


Figure 7: expanded view of top of stroke from downhole instrument

### Sinker Bar influence on Stroke Length

In the industry, it is standard practice to add sinker bars at the bottom of a rod string, above the pump, to ensure any compression in the rod string is absorbed by the sinker bar section and to maximize the pump stroke length. This is especially important when fiberglass rods are used in the top section of the rod string.

Figure 8 is a nearly vertical well with the pump set at 11,000 feet with a horizontal departure of less than 200 feet.

Figure 9 illustrates an example of a rod string with fiberglass rods in the top section and 300 ft of sinker bars at the bottom. The top green graph represents the dynagraph measured at the surface by the controller, while the black graph below represents the pump card calculated by the controller. The intermediate graphs show the dynagraphs measured by each tool in the rod string. It is important to note that the dynagraphs measured by the tools do not display any over-travel, as this is calculated using the 1DDWE.

Figure 10 also displays both the surface dynagraph measured at the surface and the pump card calculated, with the dynagraphs measured by the downhole tools in between. In this case, 1,300 ft of sinker bars were installed. It is noteworthy in this example that the addition of more sinker bars does result in a longer pump stroke under otherwise nearly identical operating conditions. However, the pump stroke calculated using the 1DDWE still exceeds the actual observed conditions.

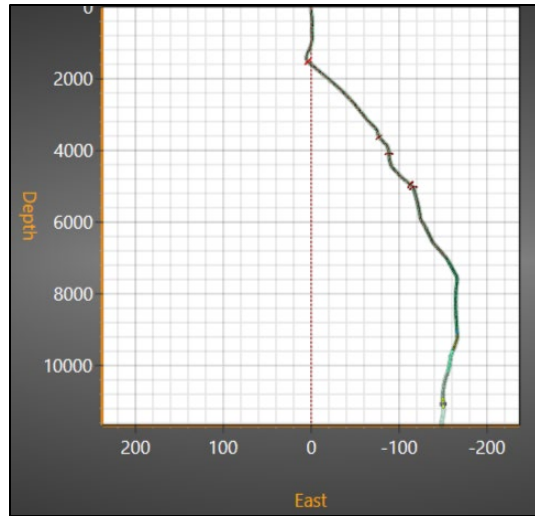


Figure 8

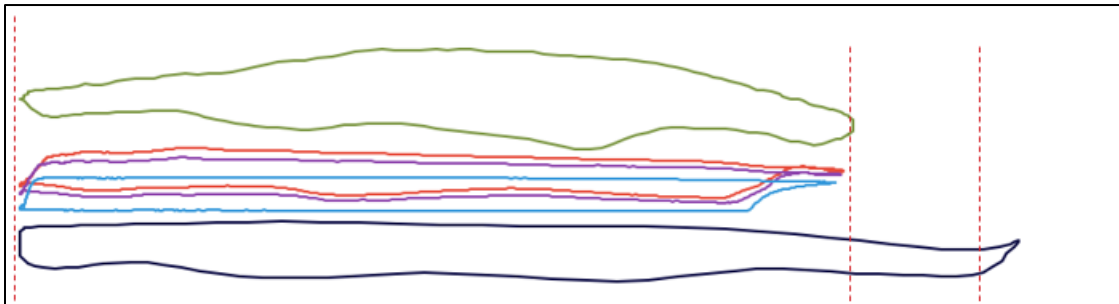


Figure 9: Stroke 126", SPM 6.87, 300ft SK Bars

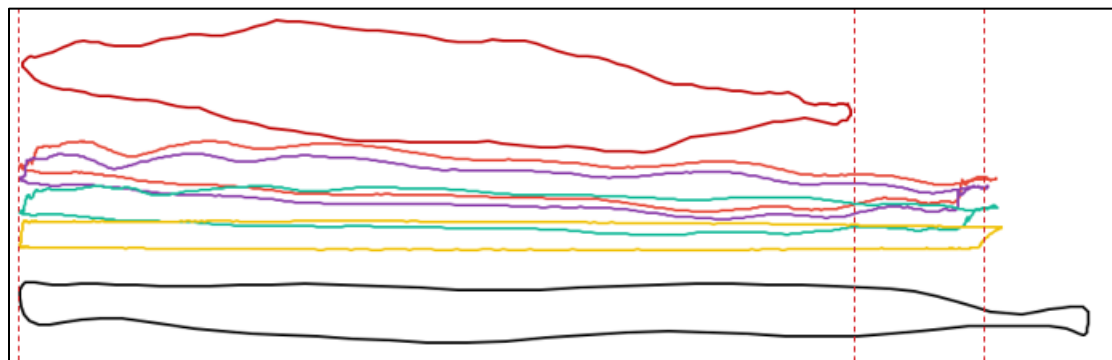


Figure 10: Stroke 126", SPM 6.87, 1,300ft SK Bars

## IMPROVED MATHEMATICAL MODEL

Gibbs<sup>4,5</sup> and others have proposed adaptations to the traditional 1DDWE which accounts for Coulomb friction. Prior to this project, these models could not be validated because relevant downhole data was not available.

Gibbs' 2011 model<sup>4</sup> – in diagnostic form - was applied to selected surface cards gathered during the project. The resulting pump cards were compared to the measured pump cards.

A team was assembled to evaluate the model results. The team used these comparisons to inform model modifications with the goal of improving the match quality. All aspects of the model were reconsidered. For most aspects, the team returned to “first principles” to validate and/or improve the Gibbs model.

## New Model Overview

The revised model is different from the 2011 Gibbs model in the following ways:

- The model accounts for phenomena not previously considered
- The friction model has been revised
- Gravitational and buoyant forces are treated differently
- Boundary conditions are handled differently

The model implementation reflects an improved understanding of the influence of rod guides on the dynamic system. This understanding was derived from tests performed during the project.

In addition, a (patent pending) process was developed to systematically derive each of the tuning factors used in the model. This process greatly simplifies the task of commissioning and maintaining integrity of the model – especially when it is incorporated into field controllers.

The validated model was then reformulated to support the predictive case, in this form, the model can be used to predict surface and pump cards – given well information and pumping unit motion profile.

Model consistency was verified. The predictive model was used to generate a pair of surface and pump cards for specific well designs. The surface cards from the predictive model were then processed by the diagnostic model and the resulting pump cards were compared to the pump cards derived by the predictive model.

## Model Results

In its current state, the diagnostic form of the model produces realistic approximations of the measured pump cards.

Figure 11 depicts the deviation survey for test subject well A. During the test, the pump was set at about 9900 ft TVD.

Figure 12 illustrates the measured downhole card from just above the pump (A) and the modeled pump card (B) for a stroke of well A at about 5.8 strokes per minute (SPM).

Figure 13 illustrates the similarity between the modeled card and the measured card.

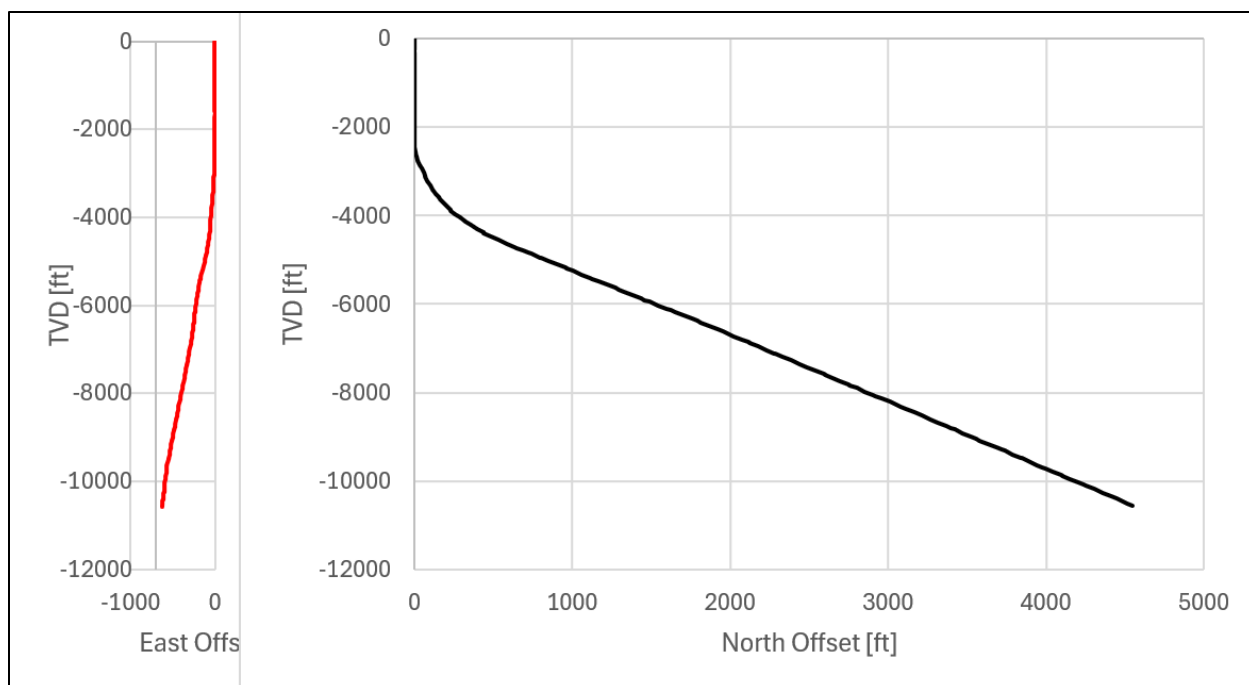


Figure 11: Deviation survey for subject well A

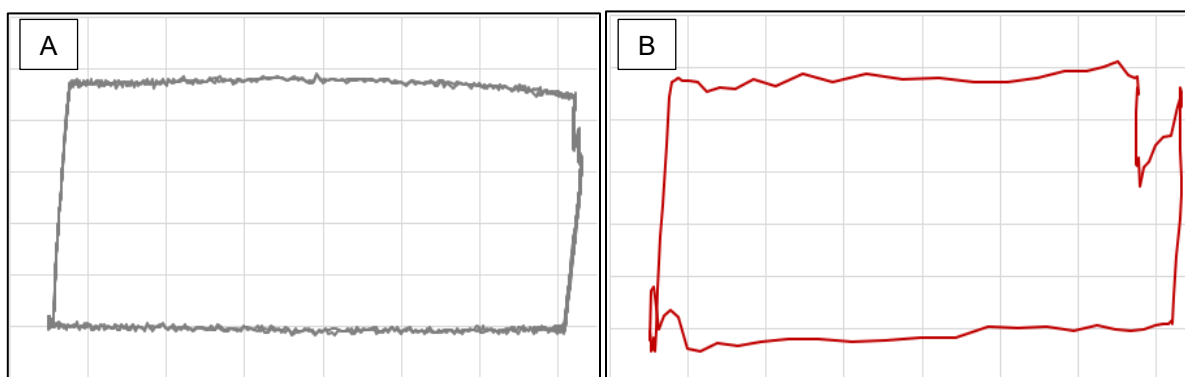


Figure 12: Measured pump card (A) and modeled pump card (B) from a stroke of subject well A

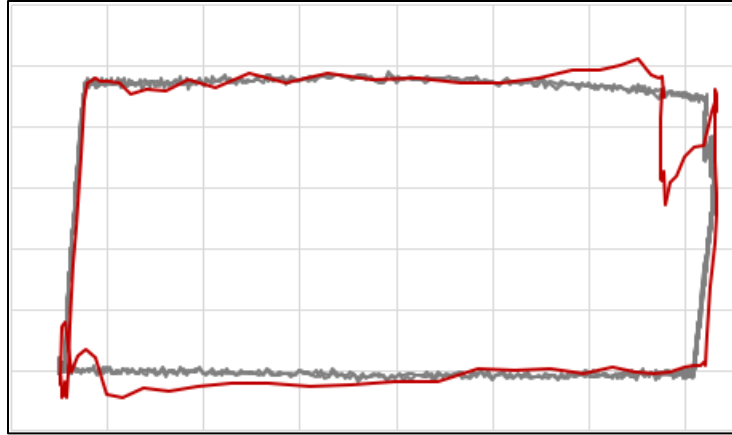


Figure 13: Measured vs modeled pump card – Well A

## Model Benefits

Industry practitioners are aware that the 1DDWE cannot produce an accurate pump card in a well with non-vertical trajectory.

The new model produces pump cards which have been verified to reasonably approximate the true behavior at the pump. Figure 14 depicts the measured pump card compared to the pump card derived by the new model and the pump card derived using 1DDWE, for the Well A.

Both modeled cards depict an (essentially) full card. In this case, control algorithms might still be able to make correct decisions from either card.

Table A quantifies the degree of match between the measured card and the two modeled cards.

Stroke length error causes error in inferred production. Errors in net stroke vs gross stroke can cause some control algorithms to make incorrect control decisions.

Fluid load error results in erroneous pump intake pressure estimates. Erroneously low pump intake pressure estimates (as would be derived from the 1DDWE card) will mask available “fluid to pump” and could lead to incorrect remediation decisions.

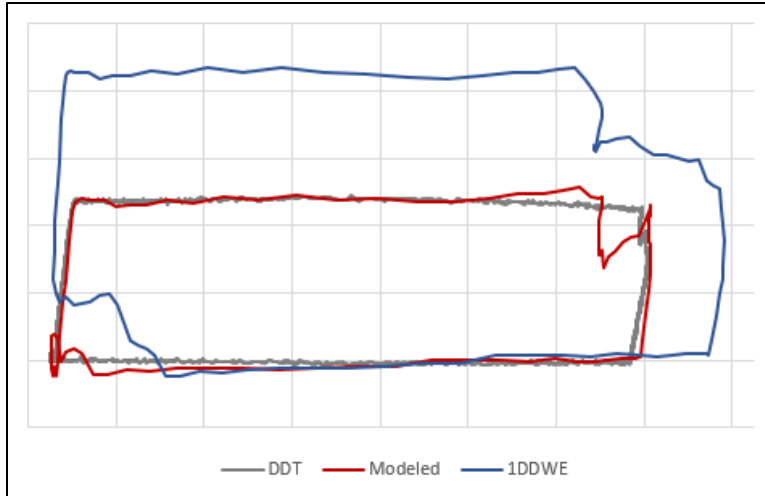


Figure 14: Comparison of modeled to measured pump cards

Table A: Percentage match between modeled and measured pump cards in Figure 14

	Damped Wave Equation % Difference	New Model % Difference
Stroke Length	12%	0.02%
Fluid Load	76%	1%

Figure 15 illustrates a gas interference card for the same well (test well A). Automated analysis of the measured downhole card results in a pump fillage fraction of 65%.

In addition to overestimating fluid load and gross stroke length, the 1DDWE card presents difficulties for pump fillage algorithms. Arguably, a pump fillage algorithm – analyzing the 1DDWE card - would likely derive a gross stroke length which is 14% too long and a pump fillage fraction of 83%.

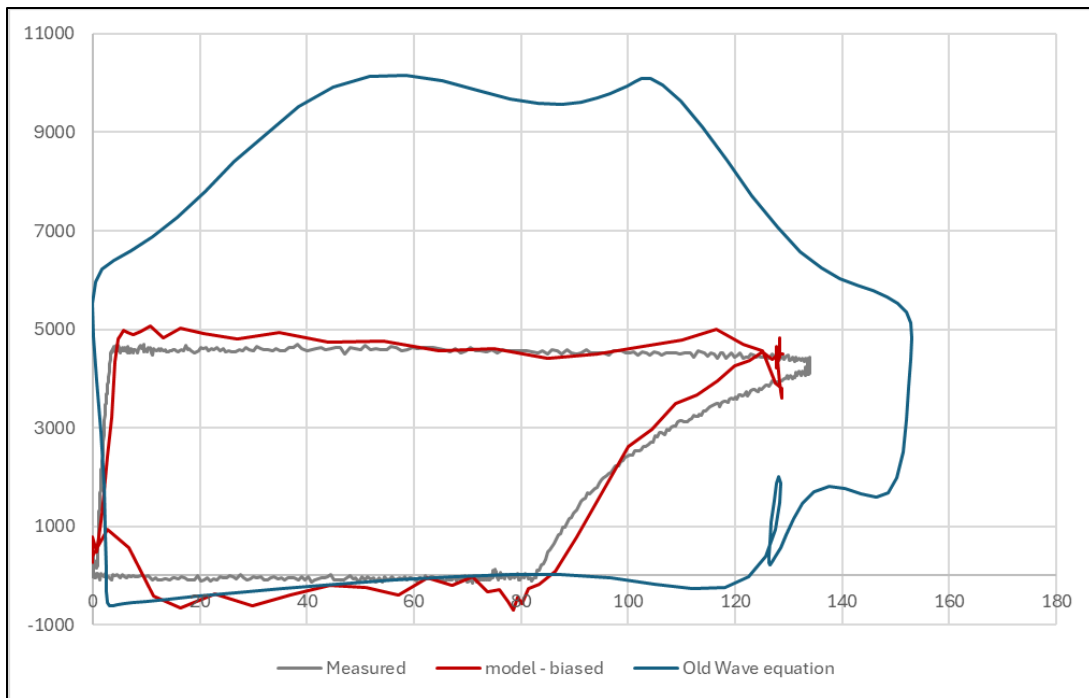


Figure 15: pump cards from gas interference stroke from well A

The same algorithm would most likely derive a gross stroke which is nearly the same as the measured card and a pump fillage fraction of 65% - very close to the measured pump fillage fraction.

From the examples presented here, it should be clear that the new model has potential benefits of:

- Improved fluid load estimation – leading to more realistic estimates of pump intake pressure and available fluid to pump.
- Improved gross stroke and net stroke estimation– leading to more realistic estimates of pump fillage fraction

As a result, a controller utilizing this new model would be more likely to make correct control decisions on a well with significant Coulomb friction.

Additionally, the card shapes produced by the new model are more characteristic of classical pump card shapes. This facilitates improved classification quality when pattern matching, neural networks or other AI/expert systems are used to classify pump cards. A human expert would have some difficulty classifying the 1DDWE card in Figure 15. It seems unlikely that any automated pattern matching logic or “artificial intelligence” would properly classify this card. For example, while a human expert might classify the 1DDWE card in Figure 15 as a “partially filled” card this human would not be able to determine whether the partial fillage was due to “pump-off” or gas interference. However, the lower-right corner of the card from the new model in Figure 15 clearly indicates gas interference.

## ALWAYS ADVANCING

The new model as described provides tighter integration between data acquisition and downhole calculations, a pump card is generated in “near real time”. This facilitates more accurate control decisions which can be made sooner after the end of each stroke. This model will continue to evolve as downhole tools are run in progressively more complicated and deviated wells.

## ACKNOWLEDGEMENTS

We wish to acknowledge ConocoPhillips for their generous support in making the wells available and funding the workover operations necessary to run the tools.

We would also like to express our sincere gratitude to Professor Dr. Gorgio Bornia from Texas Tech University for his invaluable mathematical expertise and guidance. Without his contributions, the development of this updated mathematical model would not have been possible.

A special thank you extended to Mike Poythress of ConocoPhillips, whose personal guidance, mentorship, and unwavering support have been instrumental to the success of this project to date

## REFERENCES

1. Gibbs, S.G.: "Predicting the Behavior of Sucker Rod Pumping Systems". JPT. July, 1963
2. Mills, T.M. (2014). Method for Measuring Leakage Rate and Inferring Production Rate of an Oilfield Downhole Pump. U.S. Patent 8,849,594 B2. Washington, DC.: US.
3. John Patterson, Kyle Chambliss, Lynn Rowlan, Jim Curfew: "Progress Report #4 on "Fluid Slippage in Down-Hole Rod-Drawn Oil Well Pumps", SWPSC, Lubbock, Texas (2007)
4. Gibbs et al. (2011). Apparatus for analysis and control of a reciprocating pump system by determination of a pump card. U.S. Patent 8,036,829 B2. Washington, DC: U.S.
5. Lukasiewicz, S.: "Computer Model Evaluates Oil Pumping Units in Inclined Wells", Journal of Canadian Petroleum Technology. Nov-Dec, 1990, Volume 29, No. 6.